Maximum Spectrum of Continuous Wavelet Transform and Its Application in Resolving an Overlapped Signal

Lu Xiaoquan,* Liu Hongde, Xue Zhonghua, and Zhang Qiang

Department of Chemistry, Northwest Normal University, Lanzhou 730070, China

Received December 23, 2003

To estimate the number of peaks and to find the individual peak positions in an overlapped signal, a new method called maximum spectrum of continuous wavelet transform (MSCWT) was developed by extracting the maximum coefficients of continuous wavelet transform (CWT). The peak position in MSCWT was the same as that in its original signal. In this process, CWT was performed not on a single dilation but on an appreciation dilation range. To obtain such a range, a new criterion was introduced to choose a center dilation, which was used to form the dilation range. If *Cdilation* denoted the center dilation, the proper dilation range was [*Cdilation* -6 ± 2, *Cdilation* $+1 \pm 1$]. The *Mexican Hat* function was an analytical wavelet. Utilizing the information of the peak number and the position detected by MSCWT, a fitting route was performed to recover the original signal. One simulated and four true overlapped signals, including high performance liquid chromatography (HPLC), ultraviolet−visible (UV) spectrum, and differential pulse voltammetric (DPV), were processed, and the results indicated that MSCWT could detect an overlapped peak number and position, and the curve fitting based on information of MSCWT had a higher accuracy. The proposed method was an efficient one in resolving different types of overlapped signals.

INTRODUCTION

In analytical chemistry, many instrumental methods suffer from overlapped data. Besides preventing the overlaps by chemical and instrumental methods, many mathematical means have been made to resolve overlapped signals, such as principal component regression (PCR),[1−3] the deconvolution procedure,[4,5] the derivative methods,[6,7] the fitting methods,[8] the genetic algorithm (GA),[9] immune algorithm (IA),[10,11] and many algorithms based on wavelet transform.[12−15] For those fitting methods, the achievement of a well represented fit required the knowledge of a number of component bands, their positions, shapes, and widths;[16−18] the most important values for input to the curve fitting route were the number of bands (peaks) and their positions, and the final results were often obtained by optimizing the parameters involved in the fitting functions under the supervision of the minimizing summed error. Some algorithms had been employed to detect the number of bands and their positions, such as second or fourth derivative methods.[7,19−22] Fourier self-convolution (FSD),[23] however, derivative methods required that the raw data had a higher signal-to-noise ratio (SNR). FSD involved many complicated parameter selections and it still required good SNR. In the past decade, wavelet transform (WT) had also been employed to find the individual peak position.[22−25] In Wu's paper,[25] CWT was performed on a single dilation to find positions of overlapped peaks of a square wave voltammogram (SWV) that could be described by the sech^2-function. The dilation was selected with the criterion provided in ref 26. To use a convenient description, the criterion was called "OC" in this paper. Up to now, there was no algorithm that could resolve all types of overlapped signals.

In this paper, by virtue of CWT, a novelty called MSCWT was developed, which could find each individual peak position, i.e., from MSCWT, an accurate estimate of the number of peaks and their positions could be obtained. It needed to be explained that here CWT was computed not on a single dilation but on an appreciation RANGE. The advantage of such an algorithm was facilitated by detecting different frequency overlapped peaks, here, "frequency" meant that the individual peaks overlapped each other with a different overlap degree. Using the peak information, a reliable fitting mode could be established, so the goal of resolving an overlapped signal was achieved. To find a proper center dilation so as to form an appreciation dilation range, a new criterion ("NC") was introduced, and its efficiency was compared with criterion OC. For the entire simulation procession, the noise was fully considered.

THEORY

1. CWT. For a signal $f(t)$ in time domain, its CWT could be described as eq 1

$$Wf(a,b) = \frac{1}{\sqrt{a}}\int_{-\infty}^{+\infty} f(t)\psi_{a,b}^*(t)\,dt \qquad (1)$$

where the asterisk denoted a complex conjugate, ψ was the wavelet, a was the dilation (called scale in some other place), b was the translation, and $Wf(a,b)$ was a function of a and b. If a or b were a certain constant, we could obtain the CWT under a certain dilation ($Wf_{(a)}(b)$) or CWT under a certain translation ($Wf_{(b)}(a)$).

2. Maximum Spectrum of CWT(MSCWT). When performing CWT, dilation a was used to control the dilating

* Corresponding author e-mail: luxq@nwnu.edu.cn.

10.1021/ci0342977 CCC: $27.50
Published on Web 05/29/2004

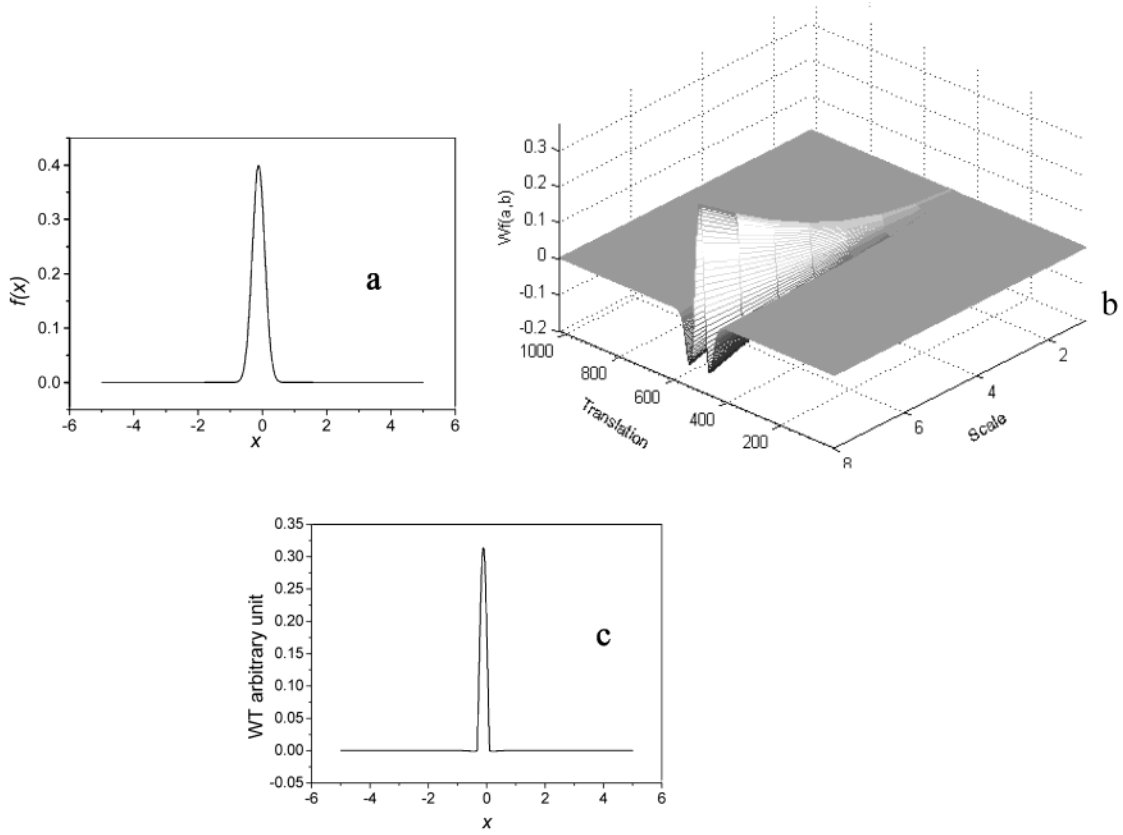

Figure 1. A simulated signal (a) and its CWT (b) and MSCWT (c).

of the mother wavelet, i.e., dilation *a* had a relationship with frequency, and this relationship could be expressed with the following eq:[27]

$$Frequency = \frac{a}{\text{the fundamental frequency of mother wavelet}}$$

If several individual peaks overlapped each other, their bulge and concave parts would have different frequency values,[1] which could be reflected in their maximum of WT. Because WT was a linear transformation, the peak positions of the data set would not change before and after WT. That is, in WT domain, the position where the WT signal had maximum was the position of the original peak, which was the base of resolving overlapping peaks with WT.

CWT on SINGLE dilation had been used to find peak positions.[25] The details procedure was as follows: (1) perform CWT of a signal on a selected dilation and obtain data $Wf_{(a)}(b)$, where *a* was the selected dilation and *b* represented the translation, and (2) detect the peaks in data $Wf_{(a)}(b)$, which were considered as peaks of the original signal. It was obvious if the original signal contained a different frequency overlapped signal; CWT on a single dilation would not detect all the overlapped peaks because the maximum of WT would appear in different dilations.[27] In this article, the dilation was let to vary in a given range to enlarge the frequency scope so as to detect all possible peaks. If CWT were performed on a dilation range, the coefficients would be three dimensions data. The proposed spectrum MSCWT was derived from the three-dimension wavelet coefficients by finding the maximum at each time (translation).

MSCWT of a signal could be obtained from the following steps: (1) choose a proper mother wavelet and an appreciated dilation range to perform CWT. (2) At every translation, detect and record the CWT maximum. (3) Plot the recorded maximum to the time, the abscissa, and the ordinate of MSCWT where the translation and the maximum, respectively, in the procedure (2) and (3) could be expressed as the pseudocode:

For ***translation****=1 to length of signal*
  For **dilation** =a1 to a2 'a1 and a2 form the range of dilation
  Find and record the maximum of ***Wf(dilation, translation)***
Next ***dilation***
Plot the ***maximum*** *to* ***translation***
Next translation

The peak position of MSCWT was the same as those in the original signal (see Figure 1). Figure 1 demonstrated the property of MSCWT. Figure 1a was a simulated signal; it had one peak, and its position was 0. Figure 1b was CWT of Figure 1a. Figure 1c was MSCWT of Figure 1a. It could be seen that the peak position in Figure 1c was in agreement with that in Figure 1a.

The proposed algorithm could avoid the mistakes of submerging or missing some useful response information.

3. Fitness Using the MSCWT Information. After acquiring peak numbers and their positions, it was easy to carry out the fitting procedure. If the number of peaks were *n*, the fitting functions could be written as follows (eq 2)

$$f_{fit}(t) = \sum_{i=1}^{n} f_i(t) \qquad (2)$$

where $f_i(t)$ was one of the following functions (eqs 2.1, 2.2, and 2.3)

$$f_g(t) = \frac{A}{W\sqrt{2\pi}} e^{-(t-t_0)^2/2W^2} \quad (2.1)$$

$$f_l(t) = \frac{2A}{\pi} \frac{W}{4(t-t_0)^2 + W^2} \quad (2.2)$$

$$f_{gl}(t) = f_g(t)R + f_l(t)(1-R) \quad (2.3)$$

where A is the peak area; t is the independent variable; t_0 is the peak position; W is the width at half-height of the peak; and R is a number between 0 and 1.

EXPERIMENT

1. Simulated Overlapped Signal. An overlapped signal (see Figure 7a) was simulated on time span[1,30] using the Gaussian function eq 3, which contained three groups of overlapped peaks; each group of overlapped peaks was formed with three single peaks by overlapping. To study the property of the proposed MSCWT, noise was added to eq 3 (SNR = 5) (see Figure 7b). The length of the signal was 3096

$$s = \Sigma \exp(-(x - a_i) \wedge 2/b_i) \quad (3)$$

where i goes from 1 to 9, the single peak position a_i was 4.5, 5, 5.5, 14.5, 15, 15.5, 24.5, 25, and 25.5, and the corresponding b_i was 0.05, 0.05, 0.05, 0.1, 0.1, 0.1, 0.12, 0.12, and 0.12. Because of the difference of value of b, each group had a different overlapped frequency. From left to right, these peaks were named with P1, P2, P3, P4, P5, P6, P7, P8, and P9.

2. Experiment of HPLC. Ten tablets of asafetida acid were ground into powder and dissolved into double distilled water. The mobile phase was a solution of HCOOH and 0.05% H_3PO_4 (1:2), and the velocity of flow was 0.8 mL/min. Daojin 2c-6A was the ultraviolet photometric detector, and the wavelength was 320 nm. The amount of the injection was 15 mL. The experiment was performed at room temperature.

3. Ultraviolet Spectrum of Complex $Gd^{3+}-Sr^{2+}-$CPA III. The ultraviolet spectrum of complex $Gd^{3+}-Sr^{2+}-$CPA III was obtained in 0.1 M $NaNO_2$ solution, pH was 5.0, the scanning rate was 400 nm/min, $\Delta\lambda = 2$ nm. The data were shown in Figure 7a with the scattered dots.

4. Voltammetric Signal. All electrochemical experiments were performed on a CHI 900 station (CH Instrumental Co. Ltd., Austin, U.S.A.) with an Ag/AgCl electrode as the reference electrode and a platinum wire as the counter electrode. All chemicals were analytical grade.

(1) For DPV of dopamine (DA) and ascorbic acid (AA), a gold disk was the working electrode, which was modified with a metal porphyrin (the porphyrin was 5-[4-(3-mercaptopropyloxyphenyl)]-10,15,20-tris(2-chlorphenyl)porphyrin, the metal was Co(II)). The supporting electrolyte was 0.1 mol/L $Na_2HPO_4-KH_2PO_4$ buffer solution (pH = 6.60), scanning rate 50 $mV \cdot s^{-1}$. The original signal was shown and marked with "O" in Figure 10a. Because DA and AA had a close oxidization potential, DA interfered with the determination of AA in the electrochemical experiment. DPV of a mixture of AA and DA was an overlapped signal.

(2) Pb^{2+} and Cd^{2+} were determined simultaneously using DPV in 0.1 mol/L HCl solution. A carbon/glass electrode was used as the working electrode. The obtained DPV plots were displayed with "◇" in Figure 11a, and the concentration of Pb^{2+} and Cd^{2+} was 5.0×10^{-5} and 1.0×10^{-6} mol/L, respectively.

5. Computations Experiments. All computations were carried out by using the program developed by us with Microsoft Visual Basic 6.0 in a Microsoft 98 environment on a PC with a Pentium III processor. CWT were performed with Wavelet Toolbox 2.0 of MATLAB Version 6.0 (The Math Works Inc., MA).

RESULTS AND DISCUSSION

1. Selection of the Analyzing Wavelet. Although many wavelet functions could be the analytical wavelet to run CWT, in practice, the analytical wavelet was required to have a better resolution. In this paper, the appreciation wavelet was chosen from many types of wavelets (*Coiflets5 (Coif5), Mexican Hat (mexh), Morlet (morl), Biorthogonals4.4 (bior 4.4), Haar wavelet, Daubechies8 (db8), Daubechies6 (db6), Symlets4 (sym4), Symlets8 (sym8), Coiflets2 (coif2)*). For an overlapped signal, keeping other conditions the same, when using a different wavelet, the MSCWT would be different, which could be seen in Figure 2. Figure 2a was an overlapped signal simulated with eq 4

$$f(x) = \frac{1}{\sqrt{2\pi}} e^{-(x-5)/(2\times 0.2)^2} + \frac{1}{\sqrt{\pi}} e^{-(x-4.6)/(2\times 0.2)^2} \quad (4)$$

$$R = \frac{x_2 - x_1}{0.5(Y_1 + Y_2)} \quad (5)$$

where x_1 and x_2 are the peaks positions, Y_1 and Y_2 are the bottom widths of the two peaks, and R is degree of separation.

In Figure 2a, there were two peaks, of which the positions were 4.6 (P1) and 5.0 (P2), respectively. The degree of separation R was 0.59.

Parts b−k of Figure 2 were MSCWT of Figure 2a using coif5, *mexh*, *morl*, *bior 4.4*, *haar*, *db8*, *db16*, *sy4*, *sym8*, and *coif2* as wavelet functions, respectively. To compare, CWT was carried out in the same dilation range (from 1 to 8). Among them, only Figure 2c, in which *mexh* as the analytical wavelet, could display the correct peak positions; the positions of P1 and P2 were 4.62 and 5.03, respectively, and the relative errors were 0.43% and 0.60%, which were consistent with the property of eq 4. As seen in Figure 2, MSCWT based on other wavelets could not detect the exact peak number and positions. In Figure 2e,h,i,k MSCWT did not show the correct peak number, and in Figure 2b,d,g,j there were some spikes, which interfered the peaks finding. So the *mexh* function was chosen as the analytical wavelet.

2. Selection of an Appreciate Dilation Range. To get MSCWT with a higher resolution, an optimized dilation range was needed to perform CWT, i.e., a proper bottom and top dilation of the range should be found. But there was not a valid method of obtaining them straightly. In this paper, first, a proper dilation was selected as the center dilation,

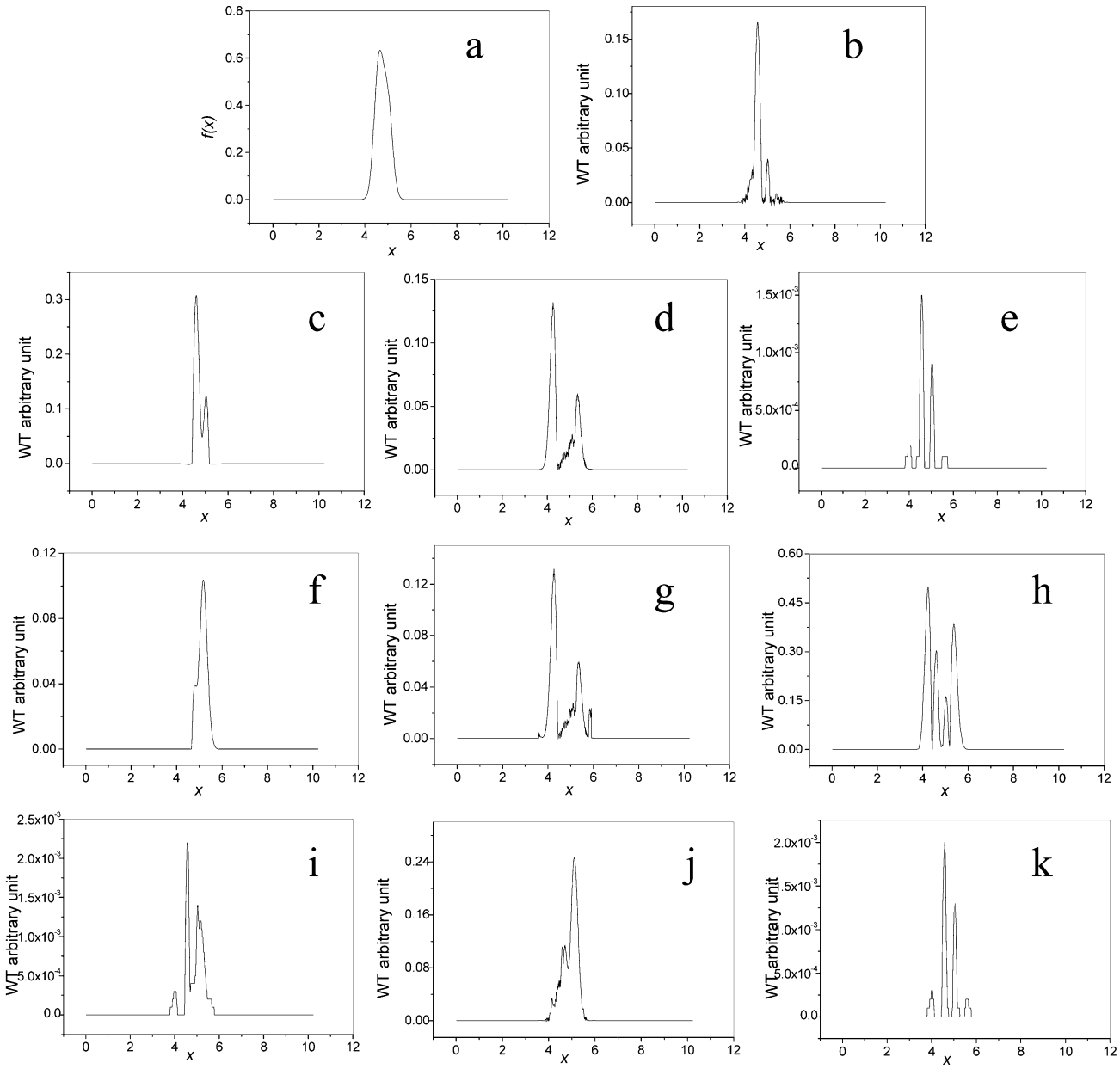

Figure 2. An overlapped signal (a) and its different MSCWT obtained by using a different wavelet function (b) *coif5*, (c) *mexh*, (d) *morl*, (e) *bior 4.4*, (f) *haar*, (g) *db8*, (h) *db16*, (i) *sym4*, (j) *sym8*, and (k) *coif2*.

and then the bottom and top dilations were constructed by shifting the center dilation toward the negative and positive, respectively. Thus there were two problems encountered: one was how the center dilation was selected, and the other was how much the dilation should be added or subtracted to get the top or bottom dilation. For the first one, criterion NC was introduced to search for the center dilation. The second problem was discussed in part 2.2.

2.1. Selection of the Center Dilation. Here the center dilation was hoped to have both a higher resolution and a better smoothing degree.

Criterion OC could be written as eq 6:

$$influence(a) = \sum_{b=1}^{length(f(x))} [(dWf(a,b)/db)]^2 \qquad (6)$$

Equation 6 indicated the influence resulting from dilations on the alteration of $Wf(a,b)$ with respect to translations. The dilation caused the cumulative alteration of $Wf(a,b)$ versus translation toward a minimum to be the best dilation. However, according to the report,[26] the minimum of *influence*(a) could only indicate the minimal value of a cumulative alteration of $Wf(a,b)$ with respect to translation, not completely denoting the degree of curve smoothing; moreover the smoothing degree did not have a direct relationship with resolution, so if one hoped to choose an appreciation dilation with a higher resolution, it was obvious that the criterion OC did not adapt to him/her.

In this paper, the introduced criterion (NC) could be represented with eq 7

$$fitness(a) = \sum_{b=1}^{length(f(x))} [|Wf(a,b)| - |f(b)|]^2 \qquad (7)$$

As could be seen *fitness*(a) represented the cumulated difference between the wavelets coefficients ($Wf(a,b)$) and

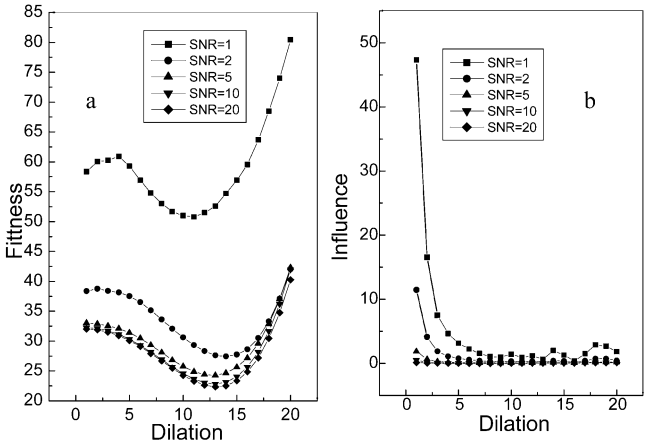

Figure 3. Selected the center dilation for the signals with different SNR using criterion NC (a) and criterion OC (b).

Table 1. Proper Dilation for the Signal with Different *S*/*N*

SNR	criterion NC	criterion OC
1	11	16
2	14	16
5	12	8
10	13	8
20	13	7

the original data at each transition, i.e., the value of *fitness*(*a*) represented the resemble degree between CWT and the original data. The dilation which made the *fitness*(*a*) have the minimum would be chosen as the best dilation.

To test the capability of the proposed criterion, a series of overlapped signals with different SNR was simulated with eq 8

$$f(x) = \frac{1}{\sqrt{2\pi}} e^{-(x-5)(2\times 0.2)^2} + \frac{1}{\sqrt{\pi}} e^{-(x-4.45)/(2\times 0.2)^2} + noise(x) \quad (8)$$

$$noise(x) = \frac{(0.5 - \mathrm{RND}_x)\max}{S/N}$$

where SNR is the ratio of signal-to-noise; max is the maximal value of the original signal, and RND_x is the random number between 0 and 1.

To compare, the best dilations were selected with the two criterions. *mexh* was used as the analytical wavelet. Figure 3 exhibited the values of the *fitness*(*a*) and *influence*(*a*) for the simulated signal with different SNR. The best dilations were shown in Table 1.

As was seen from Table 1, for both criterions, the selected best dilation changed with SNR. With the decrease of SNR, the dilation selected by criterion OC became greater, but by criterion NC, the dilation became smaller. When the SNR level was the same, two criterions gave two different results. When SNR was low, criterion OC gave a greater dilation value, while criterion NC gave a smaller value relatively. When SNR was high, the results were contrary to the previous results. When SNR became greater, the curves in Figure 3(b) became straighter_which made it difficult to find the minimum value to select the best dilation, but the curves in Figure 3(a) indicated that the value of *fitness*(*a*) was sensitive to the transform dilation and there was always a concave point, which made it easy to obtain the appreciation dilation.

In the above-mentioned, criterion OC did not count factors of the original signal; therefore, sometimes, its selection was not the best one, and the WT on such a dilation certainly had a poor fitting. Criterion NC was the criterion that was widely used in the least-squares fitting; WT on the dilation selected by it, in fact, was a wavelet curve fitting for the signal in the condition of the minimizing error. Figure 4 showed an example comparing the difference of two criterions.

An overlapped noised signal was generated with eq 8 (SNR = 10) and shown in Figure 4a. For the signal, the best dilations chosen with criterion NC and OC were 13 and 8, respectively. In Figure 4b, curve 1 was CWT on dilation 13 and curve 2 on 8. As could be seen, curve 1 displayed two peaks clearly; however, in curve 2, for its poor smoothing, the peak numbers and their positions were not easy to read, which indicated that criterion NC was superior to criterion NC in obtaining better resolution and fitting.

So criterion NC (eq 7) was used to select the center dilation.

2.2. Selection of Appreciation Dilation Range. After finding the center dilation, the next step was to construct the top and bottom dilation to form a dilation range. In this paper, a proper number was subtracted from the center dilation to form the bottom dilation, and a proper number was added to form the top dilation. Figures 5 and 6 exhibited eight different MSCWT of a signal on a different dilation range. The signal was simulated with eq 8 (SNR = 5). In Figure 5, the top dilation was locked at 10, and the bottom dilations were as follows: $a = 1$, $b = 3$, $c = 6$, $d = 9$. With

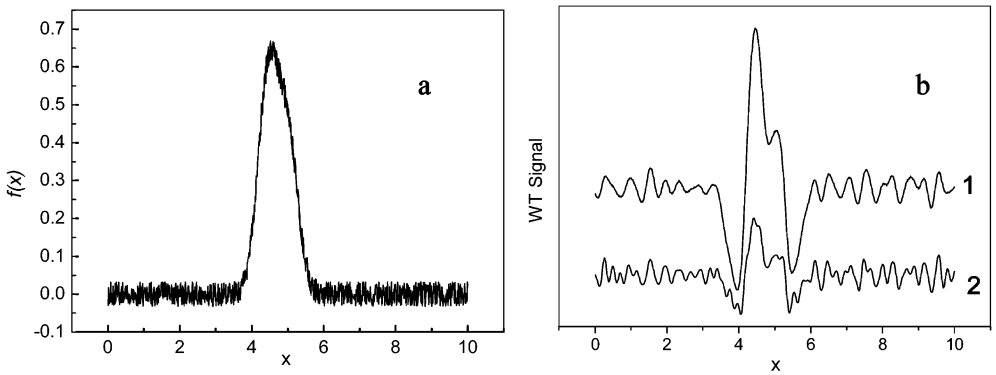

Figure 4. (a) A simulated overlapped signal with eq 8 (SNR = 10) and (b) CWT curves on two different dilations; for curve 1, dilation was 13, and for curve 2, dilation was 8.

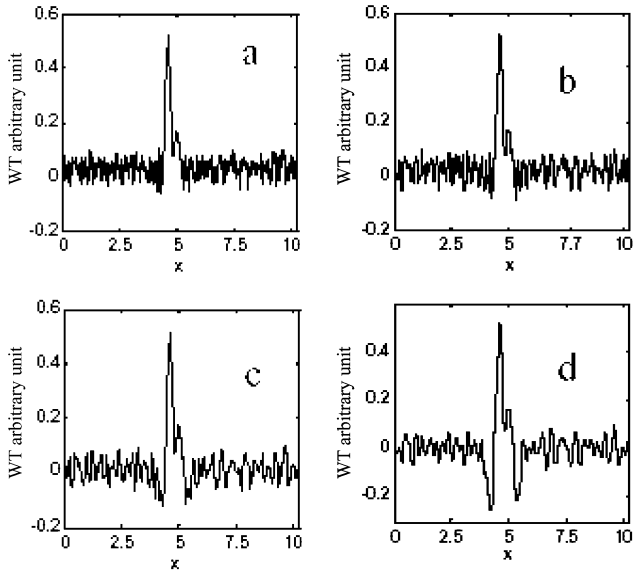

Figure 5. Affect of bottom dilation of range on MSCWT: (a) [1−10], (b) [3−10], (c) [6−10], and (d) [9−10].

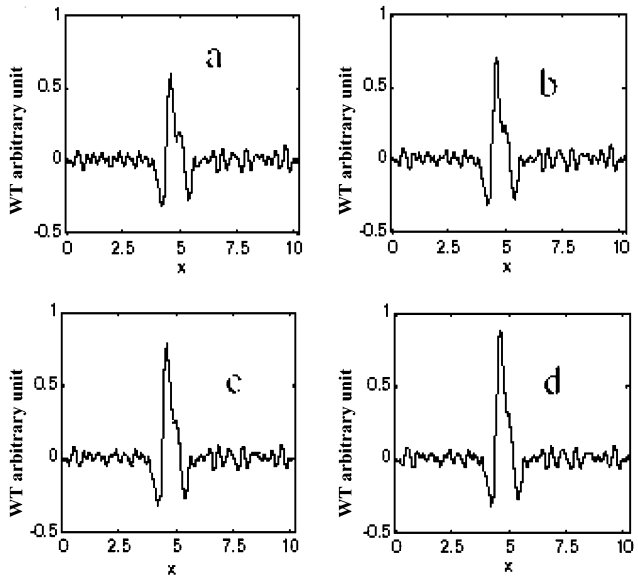

Figure 6. Affect of top dilation of range on MSCWT: (a) [10−11], (b) [10−12], (c) [10−13], and (d) [10−14].

the increasing of the bottom dilation, the interference of noise in MSCWT became light. Because the bottom dilation was correlated with the high-frequency information, the selection of the bottom dilation should depend on the level of noise. If the signal was noised seriously, to enhance the ratio of signal-to-noise, a higher dilation should be used, but it should be not more than the center dilation; if the original signal was free of noise, the bottom dilation could be 1.

For selection of the top dilation, the first considered factor should be the resolution of MSCWT. The more the dilation was, the lower the MSCWT resolution was; the second factor was to enlarge the frequency scope to cover all overlapped bands or components. In Figure 6, the bottom dilation was locked at 10, and the top dilations of subplots a, b, c, and d were 11, 12, 13, and 14, respectively. As could be seen (Figure 6c,d), when the top dilation was 13 or 14, the corresponding MSCWT had lost the resolution for the overlapped signal. After many experiments, a thumb rule could be concluded to establish the range, it was, for a noised overlapped signal (SNR < 10), if *Cdilation* denoted the center dilation, the proper dilation range could be the range [*Cdilation* -6 ± 2, *Cdilation* $+1 \pm 1$].

According to the above discussion, the whole process of resolving overlapped signals could be accomplished with the following steps:

(1) Choose the center dilation with criterion NC and establish a dilation range ([*Cdilation* -6 ± 2, *Cdilation* $+1 \pm 1$]).

(2) Perform CWT of a signal on the established dilation range and obtain MSCWT by extracting the maximum of CWT coefficients (*Mexh* as the analytical wavelet).

(3) Obtain peaks number and positions from MSCWT and fit the signal using this known information.

3. MSCWT for Simulated Signals. An overlapped signal and its noised signal (SNR = 5), which were simulated with eq 3, were exhibited in parts a and b of Figure 7. Parts c and d of Figure 7 were their MSCWT, respectively, the center dilation was 12, and the dilation range was [4, 14]. In parts c and e of Figure 7, the designed overlapped peaks all had been detected, and the peak positions were very consistent with those in the original signal (see Table 2). Parts d and f of Figure 7 were CWT of parts a and b of Figure 7 on dilation 8, 9 respectively, which were selected with criterion OC. The theoretical peak positions and the detected results with MSCWT and CWT were listed in Table 2. From Table 2 and Figure 7, it could be found that MSCWT had more accuracy in finding peaks and had more magnification for the peaks height than CWT. Comparing parts c and e with parts d and f of Figure 7, it was obvious that MSCWT had more even baselines and less spikes than CWT, which made it convenient for peaks finding.

Table 2. Detected Peaks Positions with MSCWT and CWT on Single Dilation for Simulated Overlapped Signal

	P1	P2	P3	P4	P5	P6	P7	P8	P9
theoretical peaks position	4.500	5.000	5.500	14.500	15.000	15.500	24.500	25.000	25.500
				The Signal without Noise					
MSCWT (relative error%)	4.460 (−0.888)	4.987 (−0.260)	5.475 (−0.454)	14.483 (−0.117)	15.010 (0.066)	15.507 (0.045)	24.506 (0.024)	25.013 (0.052)	25.531 (0.121)
CWT on single dilation (relative error%)	4.450 (−1.111)	4.987 (−0.260)	5.523 (0.418)	14.483 (−0.117)	15.03 (0.200)	15.547 (0.303)	24.525 (0.102)	25.062 (0.248)	25.557 (0.223)
				The Noised Signal					
MSCWT (relative error%)	4.490 (−0.222)	4.997 (−0.060)	5.482 (−0.327)	14.432 (−0.469)	15.010 (0.067)	15.498 (−0.013)	24.545 (0.184)	24.935 (−0.260)	25.128 (−1.459)
CWT on single dilation (relative error%)	4.460 (−0.889)	4.985 (−0.300)	5.475 (−0.455)	14.585 (0.586)	15.059 (0.393)	15.498 (−0.013)	24.563 (0.257)	25.172 (0.688)	25.569 (0.271)

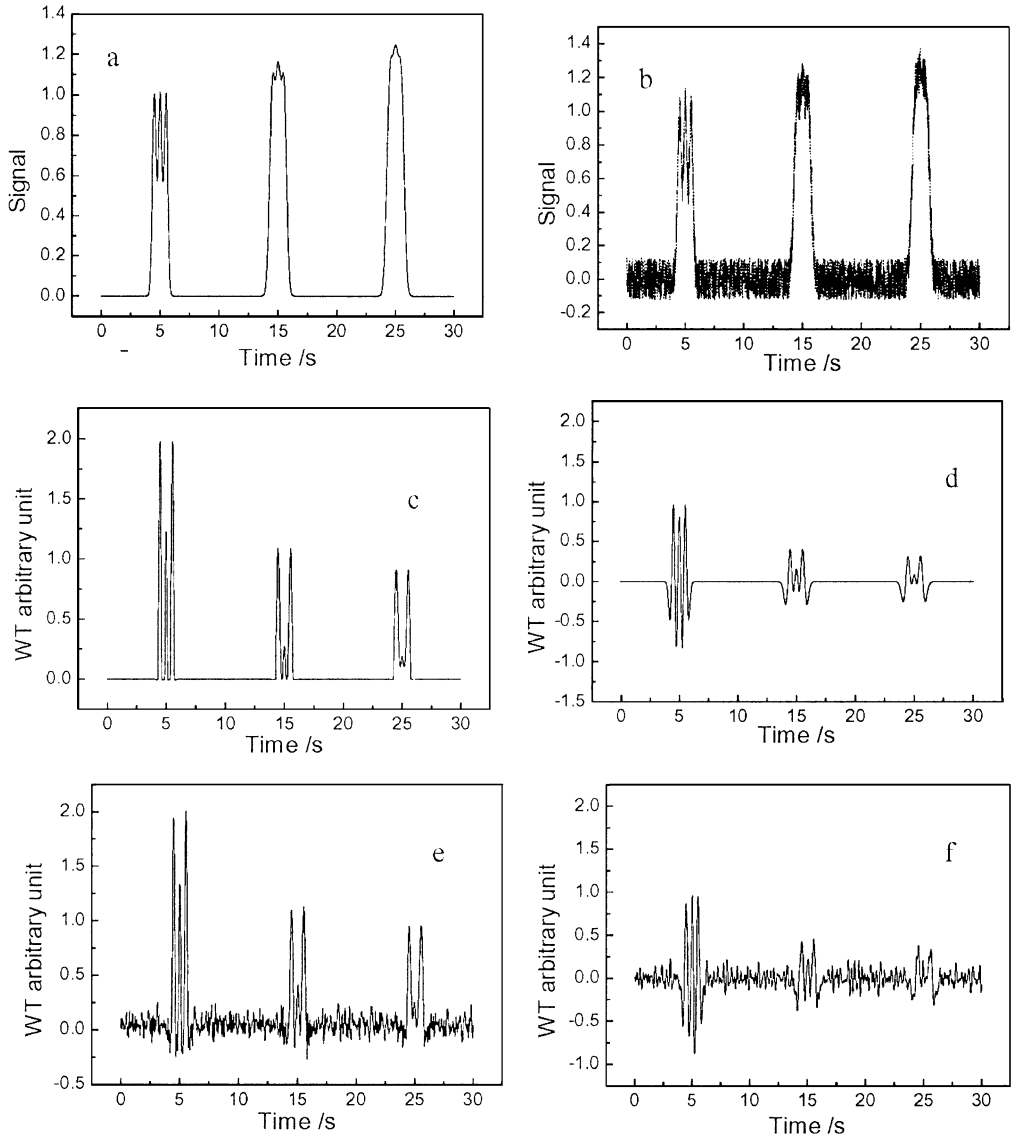

Figure 7. MSCWT for simulated overlapped signal: (a) the simulated signal without noise; (b) adding noise to Figure 7a (SNR = 5); (c) MSCWT of Figure 7a; (e) MSCWT of Figure 7b; (d) CWT of Figure 7a on dilation 8; and (f) CWT of Figure 7b on dilation 8.

4. The Processed Results of Experimental Data. 4.1. Processed Results for HPLC Signal. The HPLC was exhibited in Figure 8a. Figure 8c was its MSCWT, the center dilation was 9, and the appreciated dilation range was from 4 to 12. There were five peaks which had been detected in Figure 8c. From left to right, these peaks were named P1, P2, P3, P4, and P5. To see clearly, P3 and P4 were zoomed and shown in the top left corner. It could be seen that P3 seriously overlapped with P4 and made P4 submerge, which made it difficult to recognize its position in the original signal; however in MSCWT, their positions could be easily noted. Using the information of these positions, the original data were fitted with eq 2.2, the fitted five individual peaks signal was shown in Figure 8b and labeled with P1, P2, P3, P4, and P5, respectively, and their detailed information was shown in Table 3. In the top left corner of Figure 8b, the fitted data were plotted to the original data, the shape of the result was a line of which the slope was 1, which indicated that the fitted signal had a good resemblance with the original signal. The success of separation proved that the proposed MSCWT could exactly detect the peaks position of the overlapped signal.

Table 3. Information Obtained from the Separated Result of HPLC of Asafetida Acid

	peak area	peak position (min)	peak width at half-height (nm)
P1	0.00154	1.46090	0.12095
P2	0.00291	1.60737	0.11272
P3	0.00325	1.84979	0.26975
P4	0.00021	2.07941	0.11078
P5	0.00558	2.75779	0.13792

4.2. Processed Result for Ultraviolet Spectrum of Complex $Gd^{3+}-Sr^{2+}-$CPA III. The original ultraviolet spectrum of complex $Gd^{3+}-Sr^{2+}-$CPA III was shown with dots in Figure 9a. It could be seen that there were two peaks involved in the original signal; however, because of overlapping and noise, the accurate peak positions could not be obtained. Figure 9b was MSCWT of the spectrum. The center dilation was 28, and the transformed dilation range was from 20 to 30. In such a case, why was the center dilation higher than in another case? Because the ultraviolet signal contained more noise, to reduce the affect of noise, the higher dilation was used. As could be seen three peaks were detected in Figure 9b, which were labeled "P1", "P2", and "P3" from

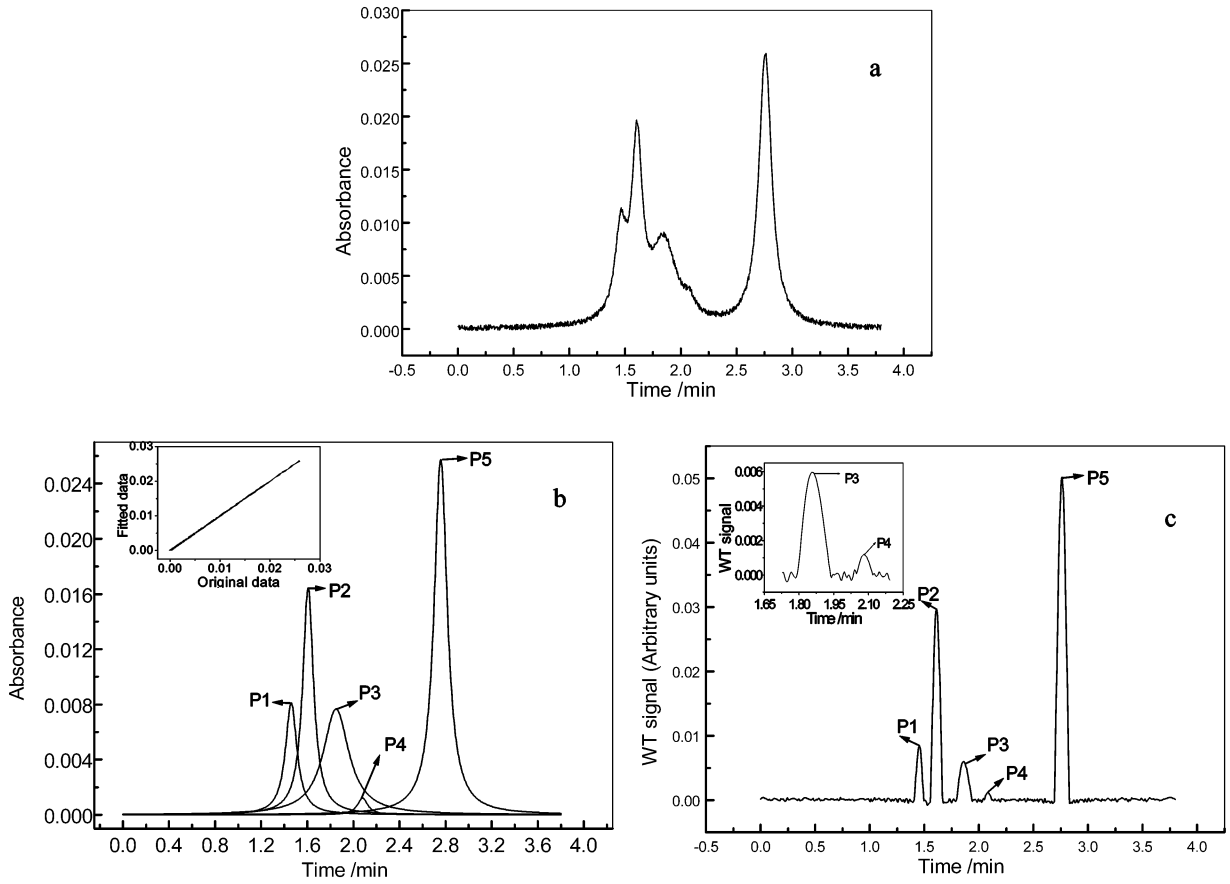

Figure 8. (a) The original HLPC signal. (b) Five separated peaks of the original HLPC signal; in the top left corner of Figure 8b, the plot of the original data to the fitted data (P1 + P2 + P3 + P4 + P5) was exhibited. (c) MSCWT of Figure 8a; in the top left corner of Figure 8c, P3 and P4 were zoomed in. The dilation range was [4, 12], and the center dilation was 9.

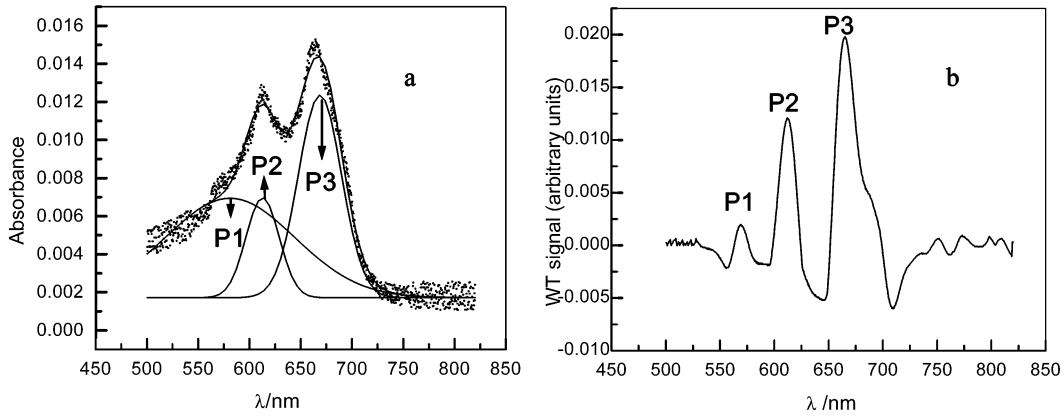

Figure 9. (a) The ultraviolet spectrum of complex $Gd^{3+}-Sr^{2+}-$CPA III and its separated peaks and (b) MSCWT of the ultraviolet spectrum of complex $Gd^{3+}-Sr^{2+}-$CPA III. The dilation range was [20, 30], and the center dilation was 28.

left to right. The positions of the three peaks were used as known information to fit, the fitted three individual peaks signals were displayed in Figure 9a. Equation 2.1 was used as the fitting function. The recovered signal (P1 + P2 + P3) was shown in Figure 9a with a solid line and without any mark. The individual peak information was shown in Table 4.

According to the above, P1 had been submerged by P2, P3, and noise, and after processing with the proposed method, it was found again. In fact, the existence of P1 was the evidence that ligand CPA III had absorption; P2 and P3 were responses to $Sr^{2+}-$CPA III and $Gd^{3+}-$CPA III.

Table 4. Information Obtained from the Separated Result of the Ultraviolet Spectrum of the Complex $Gd^{3+}-Sr^{2+}-$CPA III

	peak area	peak position, nm	peak width at half-height,nm
P1	0.820	581.121	126.072
P2	0.214	612.836	32.369
P3	0.565	668.753	42.198

4.3. Processed Result for DPV of DA and AA. An overlapped DPV signal was obtained when studying the electrochemistry reaction of DA and AA on the gold electrode modified with the metal porphyrin in our lab. The

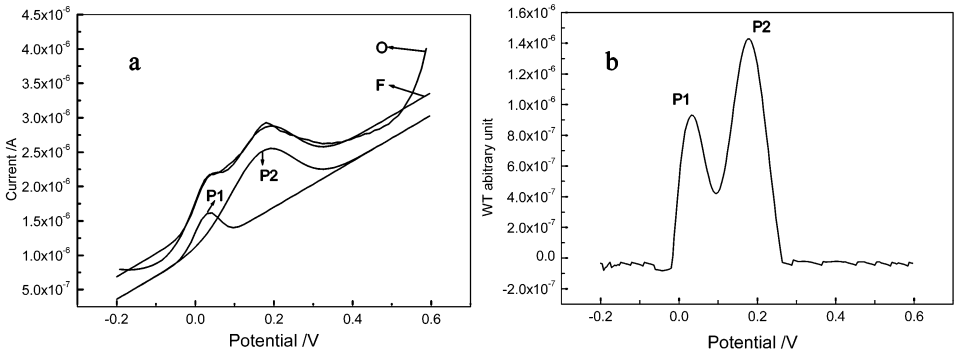

Figure 10. (a) The curve marked with "O" was DPV of DA and AA, and the one marked with "F" was the fitted signal for the DPV data; curves P1 and P2 were the fitted DA and AA individual peaks, respectively. (b) MSCWT plot, the dilation range was [1, 9], and the center dilation was 7.

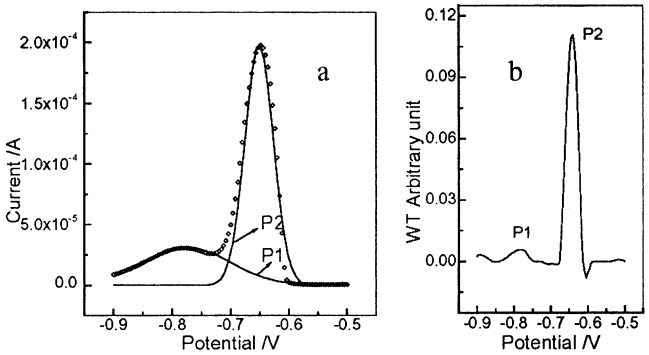

Figure 11. (a) The original DPV signal (◇); P1 and P2 were the separated peaks, which were responsive to Cd^{2+} and Pb^{2+}. (b) MSCWT of the original signal, the center dilation was 5, and the transformed range was [1, 7].

Table 5. Information Obtained from the Separated Result of DPV of Pb^{2+} and Cd^{2+}

	peak area	peak position,V	peak width at half-height, V	peak height, A
P1	5.752×10^{-6}	0.780	1.466	3.129×10^{-5}
P2	1.211×10^{-5}	0.644	0.049	1.984×10^{-4}

original signal was in Figure 10a and marked with "O". The peak shape was unsymmetrical besides overlap. Figure 10b was MSCWT of the original signal; there were two peaks (P1, P2) which could be found, and their positions were 0.036 and 0.180 V, which were responses to DA and AA. The dilation range was [1,9], and the center dilation was 7. Using knowledge of Figure 10b, the original data were fitted with a combination function, and two separated peaks were shown in Figure 10a and marked with "P1" and "P2". The recovered signal was marked with "F". It should be noted, to fit such an unsymmetrical shape, that the combination function was formed with eq 2.1 by adding a line function.

4.4. Processed Result for DPV of Pb^{2+} and Cd^{2+}. DPV of Pb^{2+} and $Cd^{2+}$was presented in Figure 11a. Figure 11b showed the MSCWT plots. The center dilation was 5, and the range was [1,7]. Two peaks P1and P2 could be found in the MSCWT plot, although P1 was very weak, by virtue of MSCWT, its position could be detected, which indicated that MSCWT was sensitive to a weak peak. Then the signal was fitted with eq 2.1, and the results were labeled "P1" and "P2" in Figure 11a. In fact, P1 and P2 were responses to Cd^{2+} and Pb^{2+}. Because of lower concentration, the response of Cd^{2+} was very weak. Moreover, Cd^{2+} and Pb^{2+} had a close reduce potential, which caused difficulty in discerning Cd^{2+} in Pb^{2+} solution. After processing with the proposed method, the above problem was resolved. The detail peaks information was listed in Table 5.

CONCLUSION

In this paper, based on the knowledge of peak numbers and positions, which were obtained by MSCWT, a fitting method was proposed to recover symmetric, unsymmetric, and noised overlapped signals in ultraviolet spectra, HPLC, DPV, and so on. MSCWT was obtained by extracting the maximum CWT coefficients. To detect different frequency peaks, here CWT was performed not on a single dilation but on a proper dilation range. Criterion NC was introduced to choose the center dilation. The processed results for simulated and experimental data indicated that the proposed method could resolve many types of overlapped signal.

ACKNOWLEDGMENT

This work was supported by the National Natural Science Foundation of China (No: 20275031, 20335030), Foundation of State Key Laboratory of Chemo/biosensing of Hunan University (No: 2002-16), KJCX-01 of Northwest Normal University, TRAPOYT of MOE, P.R.C.

REFERENCES AND NOTES

(1) Božidar, S.; Grabarić; Zorana, G.; Romà, T.; Miquel, E.; Enric, C.. Application of multivariate curve resolution to the voltammetric data factor analysis ambiguities in the study of weak consecutive complexation of metal ion with ligand. *Anal. Chim. Acta* **1997**, *341*, 105−120.
(2) Bjørn, K.; Alsberg; Andrew, M.; Woodward; Michael, K.; Winson, J. J.; Rowland; Kell, B. D. Variable selection in wavelet regression models. *Anal. Chim. Acta* **1998**, *368*, 29−44.
(3) Svante, W.; Michael, S. Chemometrics present and future success. *Chemom. Intell. Lab. Syst.* **1998**, *44*, 3−14.
(4) Jyrki, K. K.; Douglas, J. M.; David, G. C.; Henry, H. M. Noise in Fourier self-deconvolution. *Appl. Opt.* **1981**, *20*, 1866−1879.
(5) Zhang, X. Q.; Zheng, J. B.; Gao, H. Comparison of wavelet transform and Fourier self-deconvolution (FSD) and wavelet FSD for curve fitting. *Analyst* **2000**, *125*, 915−919.
(6) Leung, A. K.; Chau, F. T.; Gao, J. B. A review on applications of wavelet transform techniques in chemical analysis: 1989−1997. *Chemom. Intell. Lab. Syst.* **1998**, *43*, 165−184.
(7) Leung, A. K.; Chau, F. T.; Gao, J. B. Wavelet transform: A method for derivative calculation in analytical chemistry. *Anal. Chem.* **1998**, *70*, 5222−5229.
(8) Lu, X. Q.; Mo, J. Y. Spline wavelet multiresolution analysis for high-noise digital Signal processing in ultraviolet−visible spectrophotometry. *Analyst* **1996**, *121*, 1019−1024.
(9) Cai, W. S.; Yu, F.; Shao, X. G.; Pan, Z. X. Resolution of overlapping chromatographic peaks using a genetic algorithm. *Anal. Lett.* **2000**, *33*(2), 373−390.

(10) Shao, X. G.; Chen, Z. H.; Lin, X. Q. Resolution of multicomponent overlapping chromatogram using an immune algorithm and genetic algorithm. *Chemom. Intell. Lab. Syst.* **2000**, *50*, 91−99.
(11) Shao, X. G.; Yu, Z. L.; Sun, L. Resolution of multicomponent NMR signals using wavelet compression and immune algorithm. *Spectrosc. Acta* **2003**, *59A*, 1075−1082.
(12) Lu, X. Q.; Wang, X. W.; Kang, J. W.; Gao, J. Z. Processing discrete data for deconvolution voltammetry based on the Fourier least-squares method. *Anal. Chem. Acta* **2000**, *404*, 249−255.
(13) Shao, X. G.; Cai, W. S.; Sun, P. Y.; Zhang, M. S.; Zhao, G. W. Quantitative determination of the components in overlapping chromatographic peaks using wavelet transform. *Anal. Chem.* **1997**, *69*, 1722−1725.
(14) Lu, X. Q.; Wang, X. W.; Mo, J. Y.; Kang, J. W.; Gao, J. Z. Electroanalytical signal processing method based on B-spline wavelets analysis. *Analyst* **1999**, *124*, 739−744.
(15) Zhang, Y. Q.; Mo, J. Y.; Xie, T. Y.; Cai, P. X.; Zou, X. Y. Spline wavelet self-convolution in processing overlapped peaks in capillary electrophoresis. *Analyst* **2000**, *125*, 1303−1305.
(16) Vandeginste, B. G. M.; Galan, L. D. Critical evaluation of curve fitting in infrared spectrometry. *Anal. Chem.* **1975**, *47*, 2124−2132.
(17) Maddams, W. F. The mathematical separation of overlapping peaks: fact or fancy? *Appl. Spectrosc.* **1980**, *92*, 41−53.
(18) Gans, P.; Gill, J. B. Comments on critical evaluation of curve fitting in infrared spectrometry. *Anal. Chem.* **1980**, *52*, 351−352.
(19) Barker, B. E.; Fox, M. F. Computer resolution of overlapping electronic absorption bands. *Chem. Soc. Rev.* **1980**, *9*, 143−184.
(20) Fleissner, G.; Hage, W.; Hallbrucker, A.; Mayer, E. Improved Curve Resolution of Highly Overlapping Bands by Comparison of Fourth-Derivative Curves. *Appl. Spectrosc.* **1996**, *50*, 1235.
(21) Maddams, W. F.; Mead, W. L. The measurement of derivative IR spectra- -I, background studies. *Spectrosc. Acta* **1982**, *38A*, 437−444.
(22) Griffiths, T. R.; King, K.; Hubbard, H. V. St. A.; Schwingweill, M. J.; Meullemestre, J. Some aspects of the scope and limitations of derivative spectroscopy. *Anal. Chim. Acta* **1982**, *143*, 163−176.
(23) Jackon, R. S.; Griffiths, P. R. Comparison of Fourier self-deconvolution and maximum likelihood restoration for curve-fitting. *Anal. Chem.* **1991**, *63*, 2557−2563.
(24) Zhang, X. Q.; Zheng, J. B.; Gao, H. Curve fitting using wavelet transform for resolving simulated overlapped spectra. *Anal. Chim. Acta* **2001**, *443*, 117−125.
(25) Nie, L.; Wu, S. G.; Wang, J. W.; Zheng, L. Z.; Lin, X.; Rui, L. Continuous wavelet transform and its application to resolving and quantifying the overlapped voltammetric peaks. *Anal. Chim. Acta* **2001**, *450*, 185−192.
(26) Bjϕrn, K.; Alsberg; Andrew, M.; Woodward; Dauglas, B. K. An introduction to wavelet transforms for chemometricians: A time-frequency approach. *Chemom. Intell. Lab. Syst.* **1997**, 37, 215−239.
(27) Lu, X. Q.; Liu, H. D.; Kang, J. W.; Cheng, J. Wavelet frequency spectrum and its application in analyzing an oscillating chemical system. *Anal. Chim. Acta* **2003**, *484*, 201−210.

CI0342977